

# Emergent Criticality from Co-evolution in Random Boolean Networks

Min Liu\* and Kevin E. Bassler†

*Department of Physics, University of Houston, Houston, TX 77204-5005*

(Dated: May 19, 2021)

The co-evolution of network topology and dynamics is studied in an evolutionary Boolean network model that is a simple model of gene regulatory network. We find that a critical state emerges spontaneously resulting from interplay between topology and dynamics during the evolution. The final evolved state is shown to be independent of initial conditions. The network appears to be driven to a random Boolean network with uniform in-degree of two in the large network limit. However, for biologically realized network sizes, significant finite-size effects are observed including a broad in-degree distribution and an average in-degree connection between two and three. These results may be important for explaining properties of gene regulatory networks.

PACS numbers: 87.23.Kg, 89.75.Hc, 05.65.+b, 87.15.Aa

## I. INTRODUCTION

Boolean networks[1, 2, 3, 4, 5, 6, 7, 8] have been extensively studied over the past three decades. They have applications as models of gene regulatory networks, and also as models of social and economic systems. As “coarse-grained” models of genetic networks they aim to capture much of the observed systematic behavior of the networks while simplifying local gene expression to a binary (on/off) state[9]. Despite their simplicity, recent work has demonstrated that the model can indeed predict the essential features of the dynamics of a biological genetic circuit[10, 11]. An important feature of Boolean networks is that they have a continuous phase transition between so-called ordered and chaotic phases. It has been argued[12, 13] that gene regulatory networks of living systems should be at or close to criticality, at the so-called “edge of chaos” between the two phases, because then they can maintain both the evolvability and stability.

Many studies of critical random Boolean networks(RBNs) have considered networks with homogeneous topology in which each node has the same number of inputs from other nodes [14, 15, 16, 17, 18, 19, 20, 21, 22]. Accumulating experimental evidence[23, 24, 25], however, shows that real genetic networks do not have homogeneous connectivity, but, instead, are topologically heterogeneous. This diversity of architecture is, presumably, of great importance for the stability of living cells. Studies of RBNs with heterogeneous topology have analytically determined the location of the ordered to chaotic phase transition in the large network limit and also demonstrated how different kinds of topology affects the stability of the dynamics[26, 27, 28, 29]. These studies emphasized the importance of criticality and the influence of the network’s topology on its dynamics, but they did not attempt to explain how critical networks

with heterogeneous topology come to exist.

Recent analysis of real gene regulatory networks[30] has uncovered the possibility that the interactions between genes can change in response to diverse stimuli. The resulting changes in the network topology can be far greater than what is expected simply from random mutation. However, few general principles are known about the evolution of network topology. In an effort to determine what some of those principles may be Bornholdt and Rohlf[31] studied a simple model of neural networks known as random threshold networks (RTNs). In their study, the topology of the RTN evolved according to a rule that depends on the local dynamics of the network. According to their rule, active nodes, whose binary state changes in time, tend to lose links, while inactive node, whose binary state is fixed, tend to gain new links. They observed that with this rule for changing network topology, in the limit of large networks, the RTNs evolved to a critical network with average connectivity  $\overline{K} = 2$ . The study, therefore, discovered an interdependence between a network’s dynamics and its topology.

Motivated by these recent findings concerning gene regulatory networks and the behavior of RTNs, here we investigate the effect of a similar evolutionary rule on a simple model of a genetic regulatory system. In particular, we study an evolutionary RBN model. However, there is a fundamental difference between RTNs and RBNs. In RTNs the dynamics of each node is controlled by the same threshold function, while in RBNs the dynamics of each node is controlled by a randomly chosen Boolean function. Therefore, in addition to evolving the topology of the network, we also allow the Boolean functions used by the nodes to change. In the context of a model of gene regulation the rule we use to evolve the network topology assumes that there is some selection pressure on an individual gene due to its activity. The evolution causes genes that are in a frozen state of regulation, and, thus, are almost nonfunctional, to gain functionality, while it reduces the functionality of genes that are actively regulated. Thus this study investigates the co-evolution of network structure and network dynamics. We show that, independent of the initial topology of

---

\*Electronic address: mliu3@uh.edu

†Electronic address: bassler@uh.edu

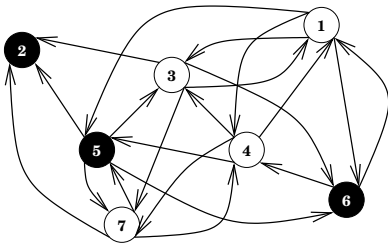


FIG. 1: A directed graph  $G(7, 3)$  represents a homogeneous RBN with 7 nodes and in-degree connectivity of 3. Black and white represent binary states ‘1’ and ‘0’ respectively. The state vector of network is  $\Sigma(t) = (0, 1, 0, 0, 1, 1, 0)$ . The arrow on each link indicates the direction of information flow in the network.

the network, the RBN evolves to a critical network with a finite number of nodes and which has a heterogeneous topology. Two different variants of our model are considered, and our principal conclusions are the same for both of them. Perhaps our most important result concerns the finite-size effects of the model. As the size of the network increases, the distribution of in-degree connectivity becomes increasingly narrow and sharply peaked at a value of  $K = 2$ . However, for biologically realized network sizes, we show that the final evolved critical state has a broad distribution of in-degree connectivity with an average value between 2 and 3. Both of these features also occur in real networks, suggesting that many of the topological features of real networks may be due to their finite size.

## II. DEFINITION OF MODEL

### A. Dynamics of Random Boolean Networks

A generalized RBN consists of  $N$  randomly interconnected nodes,  $i = 1, \dots, N$ , each of which has  $K_i$  in-degree connections from nodes that regulate its behavior. The simplest Boolean network model is a homogeneous RBN in which each node has a same number of input nodes. In this case, the connections between nodes is described by a random directed graph  $G(N, K)$  consisting of  $N$  nodes with uniform in-degree  $K$ . Figure 1 illustrates an example of  $G(7, 3)$ . Each node has a Boolean dynamical state at time  $t$ ,  $\sigma_i(t) = 0$  or 1. The state of each node at time  $t + 1$  is a function of all states of its  $K_i$  regulatory nodes at time  $t$ . Hence, the discrete dynamics of the network is given by

$$\sigma_i(t + 1) = f_i(\sigma_{i_1}(t), \sigma_{i_2}(t), \dots, \sigma_{i_{K_i}}(t)) \quad (1)$$

where  $i_1, i_2, \dots, i_{K_i}$  are those input nodes regulating node  $i$ . The function  $f_i$  is a Boolean function of  $K_i$  variables that determines the output of node  $i$  for all of the  $2^{K_i}$  possible sets of input. Note that random Boolean functions can be generated with an “interaction bias”  $p$  by

setting the output value of the function for each set of input to be 1 with probability  $p$ . The bias  $p$  can be interpreted as a biochemical reaction parameter.

Given the Boolean state of each node  $i$  at time  $t$ ,  $\sigma_i(t)$ , the state vector of network is defined as  $\Sigma(t) = (\sigma_1(t), \dots, \sigma_N(t))$ . The path that  $\Sigma(t)$  takes over time  $t$  is a dynamical trajectory in the phase space of system. Because the dynamics defined in Eq. 1 is deterministic and the phase space is finite, all dynamical trajectories eventually become periodic. That is, after some possible transient behavior, each trajectory will repeat itself forming a cycle given by,

$$\Sigma(t) = \Sigma(t + \Gamma). \quad (2)$$

The periodic part of the trajectory is the attractor of the dynamics, and the minimum  $\Gamma > 0$  that satisfies Eq. 2 is the period of the attractor.

Two phases exist in RBNs, chaotic and ordered, characterized by their dynamical behavior[3, 4]. One important way of distinguishing the two phases is to measure the distribution of its attractor periods beginning with random initial states. For RBNs in the chaotic phase the distribution of attractor periods is sharply peaked near an average value that grows exponentially with system size  $N$ , and for RBNs in the ordered phase the distribution of attractor periods is sharply peaked near an average value that is nearly independent of  $N$ . Critical RBNs, however, have a broad power law distribution of attractor periods[14].

### B. Co-evolution in Random Boolean Networks

In our model, the evolutionary changes of the topology of the network are driven by the dynamics of the network, and the functions that control the dynamics of network simultaneously evolve due to the changes in the network topology. Thus, this study investigates the co-evolution of network topology and dynamics. Similar to the one used in Ref. [31], the topology-evolving rule is simply that a frozen gene grows a link while an active gene loses a link. The dynamical functions can be changed in either an annealed or a quenched way. The detailed algorithm is defined as follows:

1. Start with a homogeneous RBN,  $G(N, K_0)$  with uniform in-degree connectivity  $K_i = K_0$  for all  $N$ , and generate a random Boolean function  $f_i$  for each node  $i$ .
2. Choose a random initial system state  $\Sigma(0)$ . Update the state using Eq. 1 and find the dynamical attractor. See the appendix for a description of the algorithm used to find the attractor.
3. Choose a node  $i$  at random and determine its av-

erage activity  $\overline{O}(i)$  over the attractor.

$$\overline{O}(i) = \frac{1}{\Gamma} \sum_{t=T}^{T+\Gamma-1} \sigma_i(t) \quad (3)$$

where  $T$  is a time large enough so that the periodic attractor has been reached, and  $\Gamma$  is the period of the attractor. If  $\overline{O}(i) = 1$  or  $0$ , then its state does not change over the duration of the attractor; it is frozen. Alternatively, if  $0 < \overline{O}(i) < 1$ , then node  $i$  is active during the attractor.

4. Change the network topology by rewiring the connections to the node chosen in the previous step. If it is frozen, then a new incoming link from a randomly selected node  $j$  is added to it. If it is active, then one of its existing links is randomly selected and removed. Note that this rewiring changes  $K_i$ .
5. The Boolean functions of network are regenerated. Two different methods have been used:
  - Annealed model: A new Boolean function is generated for every node of the network.
  - Quenched model: A new Boolean function is generated only for the chosen node  $i$ , while the others remain what they were previously.
6. Return to step 2.

The time scale for an evolutionary change of the networks, steps 2 – 6 above, is called an epoch. As we will see, using this rewiring rule the network topology evolves from a homogeneous one to a heterogeneous one. For simplicity, all random Boolean functions are generated with  $p = 1/2$ , and therefore all Boolean functions with the same in-degree are equally likely to be generated.

### III. SIMULATION AND RESULTS

We have simulated both the annealed and the quenched variants of the model. Both variants give very similar results, and our principal findings are the same for both variants. Therefore, we will present here mainly results from the annealed variant. Graph (a) of Fig. 2 shows the evolution of the average in-degree connectivity  $\overline{K} = \frac{1}{N} \sum_{i=1}^N K_i$  for networks of size  $N = 30$  in the annealed variant of the model. Four curves are shown. They show the results obtained by beginning with networks with different uniform connectivity  $K_0 = 2, 3, 4$ , and  $5$ . Each curve is the average of 15,000 independent realizations of the network evolution. This ensemble average is indicated by the angular brackets. Each different realization in an ensemble begins with a different random network and with a different random initial state vector. Remarkably, despite the difference in initial conditions, all four curves collapse after about 200 epochs, and they all approach the same final statistical steady state

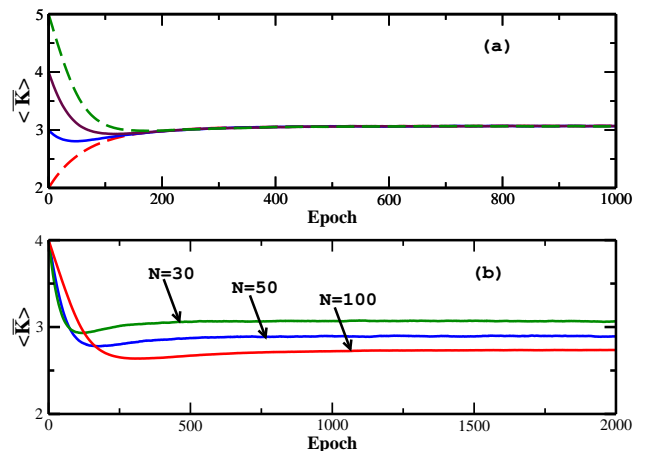


FIG. 2: (color online) (a). Evolution of the ensemble averaged in-degree connectivity in the annealed model for networks of size  $N = 30$ . The networks in each ensemble initially start from different uniform connectivity,  $K_0 = 2, 3, 4$ , and  $5$ , but reach a same statistical steady state  $\langle \overline{K} \rangle = 3.06$ . Each ensemble contained 15,000 realizations of the network. (b). Evolution of ensemble averaged in-degree connectivity for networks of three different size  $N = 30, 50$ , and  $100$  in the annealed model.

that has an average in-degree connectivity  $\langle \overline{K} \rangle = 3.06$ . This occurs without tuning and suggests that the final evolved topology of the network is independent of the initial topology of the network. The steady state value of  $\langle \overline{K} \rangle$  depends on the size of the system as shown in graph (b) of Fig. 2. Starting with networks that all have the same initial uniform connectivity  $K_0 = 4$ , but which have different size  $N = 30, 50$ , and  $100$ , we find that larger networks evolve to steady states with smaller values of  $\langle \overline{K} \rangle$ . Very similar results are obtained for the quenched version of the model. For example, for networks with  $N = 30$  the steady state value of the average connectivity is  $\langle \overline{K} \rangle = 3.08$ .

We have also calculated the in-degree and out-degree connectivity distributions,  $P(K_{in})$  and  $P(K_{out})$ , of the evolved RBNs in the steady state. Initially, all nodes of the network have a uniform in-degree  $K_0$ , meaning that the in-degree distribution is a discrete delta function  $P(K_{in}) = \delta_{K_{in}, K_0}$ , and the out-degree distribution is a binomial distribution. However, through the evolutionary rewiring of the network both the in-degree and out-degree distributions change. The in-degree and out-degree distributions in the steady state of the annealed version, are shown in Fig. 3 for  $N = 200$ . They are both right skewed bell-shaped distributions peaking at  $K = 2$ . The out-degree distribution remains a binomial distribution but the average connectivity changes. The in-degree distribution, although it has the same average connectivity as the out-degree distribution, is more sharply peaked. As the size of the network grows, the in-degree distribution becomes increasingly narrow and peaked at the value  $K_{in} = 2$ , as shown in Fig. 4. Based on this observation,

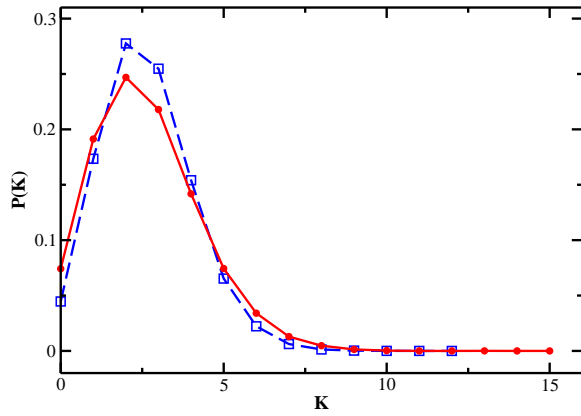


FIG. 3: (color online) Distribution of in-degree (square) and out-degree (circle) connectivity in the annealed model. The size of the networks is  $N = 200$ .

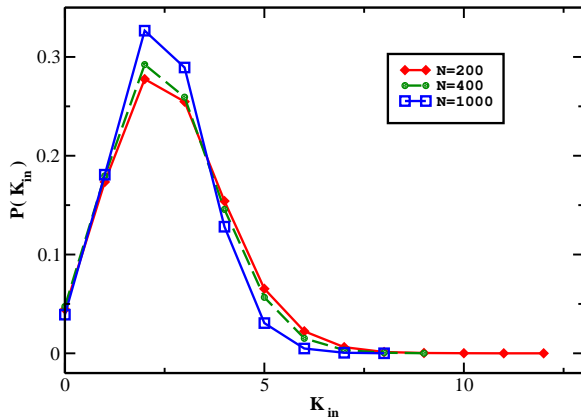


FIG. 4: (color online) Distribution of in-degree connectivity in the annealed model. The network sizes are  $N = 200, 400,$  and  $1000$ .

we conjecture that the distribution tends to converge into a discrete delta function  $\delta_{K_{in},2}$  in the large network limit  $N \rightarrow \infty$ , indicating that the network becomes a homogeneous RBN in that limit.

In order to probe the dynamical nature of evolved steady states we computed the distribution  $P(\Gamma)$  of steady state attractor period  $\Gamma$  in the ensemble of RBNs simulated. The distribution has a broad, power-law behavior for both the annealed and quenched variants of the model. Figure 5 shows the results for networks with  $N = 200$ . As long as  $N$  is about 30 or larger, results for other size networks are similar. As discussed above, this power-law distribution indicates that the networks have critical dynamics. Also in the figure, the straight line has a slope of 1.0. Thus, the critical exponent describing the power-law is approximately 1.0. This value of the exponent is obtained for all system sizes studied in both the quenched and annealed versions of the model. In short, we find that a robust criticality emerges in the

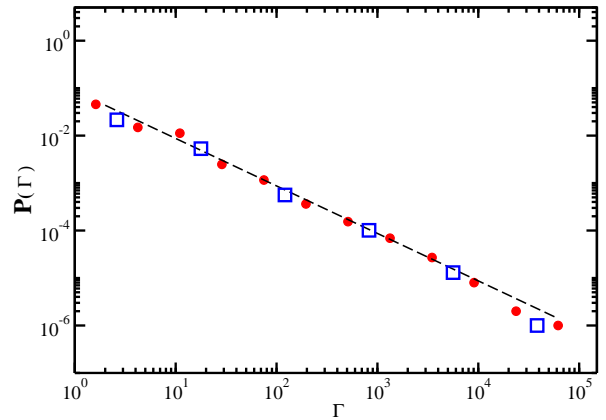


FIG. 5: (color online) Power law distribution of steady state attractor period  $\Gamma$  in both annealed (circle) and quenched (square) models for  $N = 200$  system. The dashed straight line has a slope of 1.0.

evolutionary RBNs.

Given the steady state value  $\langle \bar{K} \rangle = 2$  in the large network limit  $N \rightarrow \infty$ , we studied the finite-size effects in the model. As shown in Fig. 6, the values of  $\langle \bar{K}(N) \rangle$  for finite  $N$  obey the scaling function

$$\langle \bar{K}(N) \rangle - 2 = AN^{-\beta}. \quad (4)$$

Fitting the data to this function, we find that the coefficient is  $A = 2.50 \pm 0.06$  and the exponent is  $\beta = 0.264 \pm 0.005$ . Thus the value of  $\langle \bar{K}(N) \rangle$  is always larger than 2 for finite  $N$ . Note that steady state values of the average connectivity in random threshold networks have a similar scaling form [31], but, in that case  $A = 12.4 \pm 0.5$  and  $\beta = 0.47 \pm 0.01$ .

#### IV. DISCUSSION AND CONCLUSIONS

The mechanism we find here that leads to the emergent critical state has some similarity to self-organized criticality (SOC)[32, 33], but is different. SOC is the tendency of driven dissipative dynamical systems to organize themselves into a critical state far from equilibrium through avalanches of activity of all sizes. In our particular model, the evolutionary Boolean network is a dissipative dynamical system because multiple different states may map into the same attractor so that information is lost. Similar to SOC systems, our model is driven subject to two competing rules, and the network organizes itself into a steady state that results from a dynamical balance of the competition between those rules. Moreover, the critical state is robust irrespective of initial connectivity in both the quenched or annealed versions of the model. The emergent critical state acts like a global attractor in the evolution process. However, unlike the mechanism of traditional SOC, but similar to the mechanisms that have been shown to lead to criticality in random threshold networks [31] and in homogeneous Boolean networks

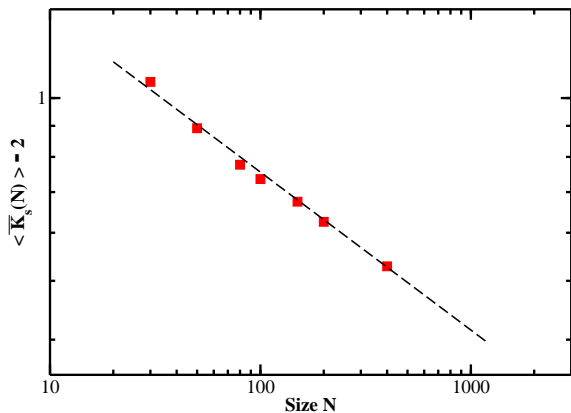


FIG. 6: (color online) Finite-size effects in the annealed model. The data shown are for systems of different sizes  $N = 30, 50, 80, 100, 150, 200$ , and  $400$ . The dashed straight line has a slope of  $0.26$ .

[20], the self-organizing mechanism here is based on a topological phase transition in dynamical networks.

Our results indicate that, with the rewiring rules we use, networks in the limit  $N \rightarrow \infty$  will evolve to have a homogeneous in-degree connectivity of 2. However, we find that finite size networks evolve to have a broadly distributed heterogeneous in-degree connectivity. The average in-degree connectivity of the evolved networks is between 2 and 3 for biologically realized network sizes. This result may be important for explaining the observed structure of real gene regulatory networks. Real genetic networks have a number of nodes  $N$  ranging from near 100 to thousands, and typically have a heterogeneous connectivity with an average in-degree slightly larger than 2. For example, a recent experiment studying the gene regulatory network of *S. cerevisiae* [30] found that the network contains 3420 genes and has an average in-degree connectivity  $\bar{K}_{in} = 2.1$ .

Finally, we note that real genetic networks exhibit an approximately scale-free out-degree distribution while the in-degree distribution is exponentially decaying[30, 34]. In our numerical study, we similarly obtain an in-degree distribution that decays faster than the out-degree distribution, but our model does not produce a scale-free like out-degree distribution. Therefore, in order to be more realistic the model needs to be extended by adding other factors that will capture this feature. We do not believe though that such extensions will alter the principal conclusions of this paper concerning the importance of finite size effects in the evolution of network topology

in real genetic networks.

## Acknowledgments

We thank Maximino Aldana, Julio Monte, Toshimori Kitami and Adam Sheya for stimulating discussions. This work was supported by the NSF through grant #DMR-0427538, and by SI International through the AFRL under contract #FA8756-04-C-0258.

## APPENDIX

In the work presented here and in our previous studies[20, 21, 22] the following algorithm was used to determine the dynamical attractor.

Begin by using the initial state  $\Sigma(0)$  as the “checkpoint” state. Then for each time  $T$ ,  $0 < T \leq T_1$ , the state is updated using Eq. 1. If  $\Sigma(T) = \Sigma(0)$ , then the attractor is found, it has period  $T$ , and the search ends. Note that the new state is compared only to the checkpoint state and no other previous states.

If after  $T_1$  updates no attractor is found then the checkpoint state is changed to  $\Sigma(T_1)$ . For each time  $T$ ,  $T_1 < T \leq T_2$ , the state is again updated using Eq. 1. If  $\Sigma(T) = \Sigma(T_1)$ , then the attractor is found, it has period  $T - T_1$ , and the search ends.

If after  $T_2$  updates the attractor has still not been found then the checkpoint state is changed to  $\Sigma(T_2)$ . For each time  $T$ ,  $T_2 < T \leq T_2 + T_{max}$ , the state is again updated using Eq. 1. If  $\Sigma(T) = \Sigma(T_2)$ , then the attractor is found, it has period  $T - T_2$ , and the search ends.

Finally, if after  $T_2 + T_{max}$  updates the attractor has still not been found then the state  $\Sigma(T_2 + T_{max})$  is used as the new checkpoint state. If  $\Sigma(T) = \Sigma(T_2 + T_{max})$ , then the attractor is found, it has period  $T - T_2 - T_{max}$ , and the search ends.

If no attractor is found after this procedure, then we stop. In this case, the average output state in Eq. 3 is calculated assuming that the attractor period is  $\Gamma = T_{max}$  and that the final checkpoint state  $\Sigma(T_2 + T_{max})$  is on the attractor.

This algorithm finds all attractors that have period less than or equal to  $T_{max}$  and that have a transient time to reach the attractor from the initial state less than or equal to  $T_2 + T_{max}$ . For the results presented in this paper we used  $T_1 = 100$ ,  $T_2 = 1000$ , and  $T_{max} = 100000$ .

[1] S. A. Kauffman, J. Theor. Biol. **22**, 437 (1969).

[2] S. A. Kauffman, Physica D **42**, 135 (1990).

[3] B. Derrida and Y. Pomeau, EuroPhys. Lett. **1**, 45 (1986).

[4] B. Derrida and G. Weisbuch, J. Phys. **47**, 1297 (1986).

[5] U. Bastolla and G. Parisi, Physica D **115**, 203 (1998).

[6] R. Albert and A. L. Barabási, Phys. Rev. Lett. **84**, 5660 (2000).

[7] M. Aldana, S. Coppersmith, and L. P. Kadanoff, in *Perspectives and Problems in Nonlinear Science*, edited by E. Kaplan, J.E. Marsden, and K.R. Sreenivasan (Springer-

- Verleg, Berlin, 2003).
- [8] B. Luque, F. J. Ballesteros, and E. M. Muro, Phys. Rev. E **63**, 051913 (2001).
- [9] S. Bornholdt, Science **310**, 449 (2005).
- [10] R. Albert and H. G. Othmer, J. Theor. Biol. **223**, 1 (2003).
- [11] F. Li, T. Long, Y. Lu, Q. Quyang, and C. Tang, Proc. Natl. Acad. Sci. U.S.A. **101**, 4781 (2004).
- [12] N. H. Packard, in *Dynamics Patterns in Complex Systems*, edited by J. A. S. Kelso, A. J. Mandell, and M. F. Shlesinger (World Scientific, Singapore, 1988).
- [13] S. A. Kauffman, *The Origins of Order* (Oxford University Press, New York, 1993).
- [14] U. Bastolla and G. Parisi, J. Theor. Biol. **187**, 117 (1997).
- [15] F. Greil and B. Drossel, Phys. Rev. Lett. **95**, 048701 (2005).
- [16] B. Drossel, Phys. Rev. E **72**, 016110 (2005).
- [17] B. Drossel, T. Mihaljev, and F. Greil, Phys. Rev. Lett. **94**, 088701 (2005).
- [18] B. Samuelsson and C. Troein, Phys. Rev. Lett. **90**, 098701 (2003).
- [19] J. E. S. Socolar and S. A. Kauffman, Phys. Rev. Lett. **90**, 068702 (2003).
- [20] M. Paczuski, K. E. Bassler, and A. Corral, Phys. Rev. Lett. **84**, 3185 (2000).
- [21] K. E. Bassler, C. Lee, and Y. Lee, Phys. Rev. Lett. **93**, 038101 (2004).
- [22] K. E. Bassler and M. Liu, in *Noise in Complex Systems and Stochastic Dynamics III, Proc. of SPIE Vol. 5845*, edited by L. B. Kish, K. Lindenberg, and Z. Gingl (SPIE, Bellingham, WA, 2005), P. 104.
- [23] D. Thieffry, A. M. Huerta, E. Perez-Rueda, and J. Collado-Vides, Bioessays **20**, 433 (1998).
- [24] T. I. Lee, N. J. Rinaldi, F. Robert, D. T. Odom, and Z. B. J. *et al.*, Science **298**, 799 (2002).
- [25] A. H. Y. Tong, G. Lesage, G. D. Bader, H. Ding, and H. X. *et al.*, Science **303**, 808 (2004).
- [26] B. Luque and R. V. Solé, Phys. Rev. E **55**, 257 (1997).
- [27] J. J. Fox and C. C. Hill, Chaos **11**, 809 (2001).
- [28] M. Aldana, Physica D **185**, 45 (2003).
- [29] M. Aldana and P. Cluzel, Proc. Natl. Acad. Sci. U.S.A. **100**, 8710 (2003).
- [30] N. M. Luscombe, M. M. Babu, H. Yu, M. Snyder, and S. A. T. M. Gerstein, Nature **431**, 308 (2004).
- [31] S. Bornholdt and T. Rohlf, Phys. Rev. Lett. **84**, 6114 (2000).
- [32] P. Bak, C. Tang, and K. Wiesenfeld, Phys. Rev. Lett. **59**, 381 (1987).
- [33] P. Bak, C. Tang, and K. Wiesenfeld, Phys. Rev. A **38**, 364 (1988).
- [34] R. Albert, J. Cell Sci. **118**, 4947 (2005).